Integrated Photonic Devices and Materials

RLE Group
Integrated Photonic Devices and Materials Group

Academic and Research Staff
Professor Leslie A. Kolodziejski, Dr. Gale S. Petrich

Graduate Students
Reginald E. Bryant, Aleksandra Markina, Eric Mattson, Sheila N. Tandon, and Ryan D. Williams

Technical and Support Staff
Cindy Lewis-Gibbs

Introduction

The emphasis of our research program is the design, epitaxial growth, device fabrication and characterization of a number of photonic and opto-electronic structures and devices. The epitaxial growth of the heterostructures is performed in the newly-installed Veeco GEN 200 solid source, dual-reactor molecular beam epitaxy (MBE) system. This MBE system is capable of the epitaxial growth of dilute nitrides and antimony-based films in addition to arsenide- and phosphide-based films. The system platens hold multiple 2”, 3" or 4" wafers, or a single 6" or 8" wafer. The system incorporates a low wobble manipulator that will enable in-situ feedback control of the epitaxial processes using optical sensors such as band edge absorption spectroscopy and spectroscopic ellipsometry.

In the following sections, the status of the various research projects will be discussed. The Riber III-V gas source molecular beam epitaxy system was utilized for the fabrication of GaAs-based devices implementing one- and two-dimensional photonic bandgap crystals within their structure, for the development of components for ultra short pulse lasers, and for the development of electromechanical optical switches. The development and simulation of rudimentary optical logic gates represents a collaborative effort between the research groups under the direction of Professors L. Kolodziejski, R. Ram and E. Ippen at MIT and Dr. S. Hamilton at MIT Lincoln Laboratory. The research projects utilizing photonic crystals in addition to the development of the optical switch represents the combined efforts of the research groups led by Professors J. Joannopoulos (Theory), L. Kolodziejski (Fabrication), H. Smith (Fabrication), and E. Ippen (Measurement). The complexity of the design, fabrication and characterization of these photonic crystal-based structures necessitates a strong interaction between the various research groups. A collaborative effort between the groups led by Professors Kolodziejski, Ippen and Kaertner has led to the development of saturable bragg reflectors that are required in ultra short pulse lasers.

1. Photonic Integrated Circuits for Ultrafast Optical Logic

Sponsors
DARPA

Project Staff
Aleksandra Markina, Ryan Williams, Dr. Gale S. Petrich, Professor Rajeev Ram, Professor Erich P. Ippen, Professor Leslie A. Kolodziejski, and Dr. Scott Hamilton

The aim of this project is to model and to produce a modular, monolithically-integrated, all-optical logic unit cell capable of performing a complete set of Boolean operations at speeds of hundreds of gigabits per second. The basic structure of the unit cell consists of a balanced Mach-Zehnder interferometer (MZI) with a semiconductor optical amplifier (SOA) in each arm, as shown schematically in Figure 1(a). The material system of choice for this project is (In,Ga)(As,P) grown on InP substrates. Components include straight ridge waveguides, ridge waveguide bends, power splitters and couplers, and semiconductor optical amplifiers. The asymmetric twin waveguide [1, 2] approach is employed for the monolithic integration of active devices with passive components. In the asymmetric twin waveguide approach, the active devices are stacked vertically on a lower passive waveguide, as shown schematically in Figure 1(b). The use of an adiabatic taper allows the optical signal to move from the passive waveguide to the active waveguide.

A set of design and simulation tools is used to develop the design rules, to identify tradeoffs, to determine fabrication tolerances, and to estimate the effects of imperfections in semiconductor processing on the device's performance. Modeling of each type of component calls for an appropriate numerical approach. The challenge is to optimize the performance of each component even when all of the components are monolithically-integrated within a photonic integrated circuit.

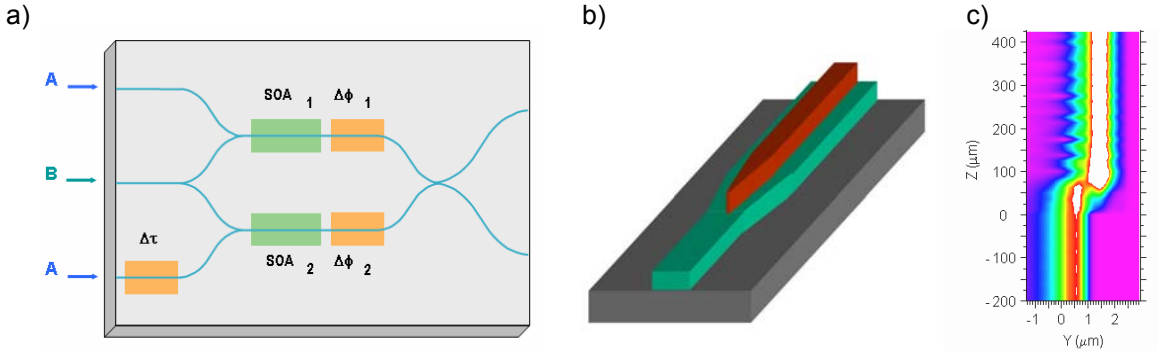

Figure 1. a) Schematic representation of the optical unit cell. b) Schematic representation of the asymmetric twin waveguide. The red active waveguide reside above the green passive waveguide. c) BPM results of the energy transfer from the lower passive waveguide to the upper active waveguide.

The beam propagation method (BPM) is suitable for simulating long devices that exhibit slow variations in the direction of propagation. BPM can be used to model components with low back reflections and beam divergence. BPM simulations are used to model passive waveguides, multimode interference couplers, and asymmetric twin-waveguide (ATG) structures with adiabatic tapers that facilitate optical energy transfer between active and passive circuit components. Figure 1(c) illustrates the energy transfer from the lower passive waveguide into the upper SOA via an adiabatic taper in an asymmetric twin waveguide structure.

Three-dimensional, finite-difference, time-domain (FDTD) calculations are highly accurate, but poorly suited for modeling full-scale devices due to large demands this method places on computational resources. FDTD simulations are used to estimate the reflections between the various components by considering a small computational domain around each abrupt interface. The FDTD computations confirm

that the reflectivity of the adiabatic tapers with blunt tips is well below 10^{-4}. Therefore, the chosen integration scheme allows for the use of SOAs as single-pass devices.

Custom MATLAB scripts are being developed to assess the tradeoffs in the SOA performance for both linear and non-linear applications in photonic integrated circuits. Methods for minimizing pattern effects are being considered. One of the goals of this work is to produce design rules that specifically address the design of the SOAs for switching applications. The phase in the SOAs is modeled in order to study cross-phase modulation in a balanced MZI with an SOA in each arm.

The first prototypes of the all-optical logic unit cell have been fabricated (Figure 2) using the facilities within the Microsystems Technology Laboratory (MTL) and the Nanostructures Laboratory (NSL). Figure 2(a) shows a completed quarter of a 2" InP wafer that contains two different styles of dies. The smaller of the two die contains a series of isolated components that will be used to confirm the device design and the computer simulation results. The larger die contains multiple optical unit cells [Figure 2(b)] and wavelength converters. Currently, both dies are being optically and electrically characterized.

a) b)

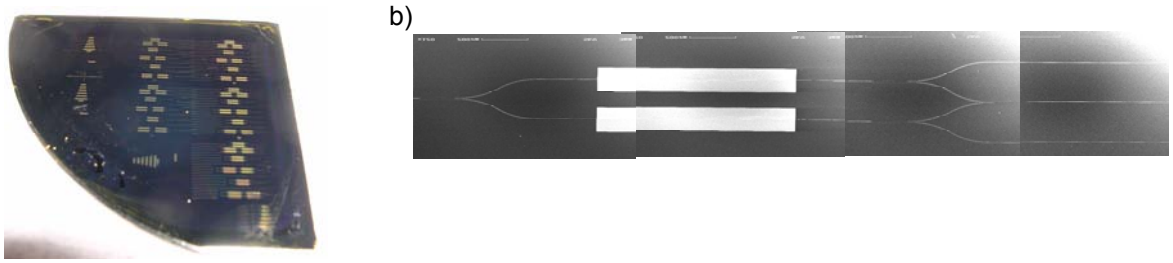

Figure 2. a) An photograph of the fabricated dies on a quarter of a 2" InP wafer. b) A composite scanning electron image of an optical unit cell.

References

[1] F. Xia, V. Menon and S. R. Forrest "Photonic Integration Using Asymmetric Twin-Waveguide (ATG) Technology Part I- Concepts and Theory" IEEE J. Selected Topics in Quantum Electronics 11(1), 17-29 (2005).

[2] V. Menon, F. Xia and S. R. Forrest "Photonic Integration Using Asymmetric Twin-Waveguide (ATG) Technology Part II- Devices" IEEE J. Selected Topics in Quantum Electronics 11(1), 30-42 (2005).

2. Broadband Saturable Bragg Reflectors for Modelocking Ultrafast Lasers

Project Staff:
Sheila N. Tandon, Juliet T. Gopinath, Hanfei M. Shen, Dr. Gale S. Petrich, Professor Franz X. Kaertner, Professor Erich P. Ippen and Professor Leslie A. Kolodziejski

Sponsor
National Science Foundation, Award Number ECS-0322740
Office of Naval Research, Contract Number N00014-02-1-0717

Modelocking ultrafast lasers require broadband mirrors with saturable absorbers. One such suitable reflector employed semiconductor absorbers that have been transferred onto broadband metal mirrors by post-processing [1]. In addition a broadband Saturable Bragg Reflector (SBR) with an epitaxially-grown AlGaAs/CaF_2 mirror and a GaAs absorber has been used in a Ti:Sapphire laser [2]. AlAs/GaAs or AlAs/AlGaAs mirrors with saturable absorbers have limited bandwidth due to the low index-contrast between the individual layers and are hence not suitable for broadband applications. An alternative approach is to monolithically integrate absorbers onto AlGaAs-based Bragg-mirrors and to use steam oxidation to convert the AlAs layers to Al_xO_y which has a lower index of refraction (n~1.6). The absorber and high index layers are selected based on the laser's wavelength. AlGaAs/Al_xO_y mirrors with InGaAs absorbers form large area broadband SBRs for infrared lasers, including Cr:Forsterite [3]. Due to the lattice mismatch to GaAs, InGaAs-based absorbers strain the structure. When thicker absorbers are used for higher saturable loss, the strain results in absorber delamination during the oxidation process. Varying the temperature profile before and after oxidation stabilizes the SBR structure. For visible wavelengths, SBRs are fabricated with InGaAlP high-index layers and GaAs absorbers. Using these oxidation techniques, SBRs with broadband reflectivities are created for lasers from the visible to infrared (Fig. 1).

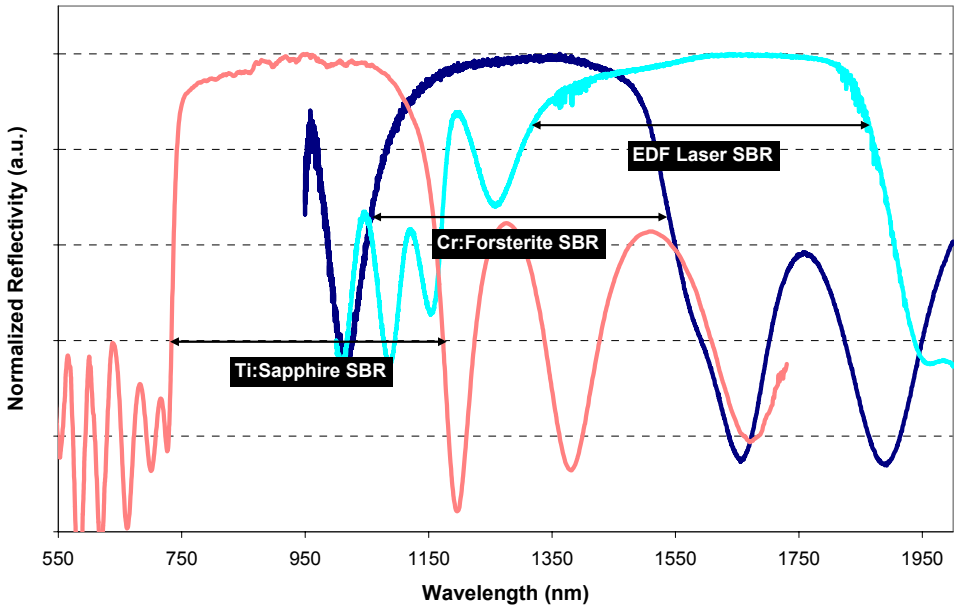

Figure 1. Reflectivity measurements of SBR structures fabricated for three different laser systems: Ti:Sapphire, Cr:Forsterite, and Er-doped fiber (EDF) laser with theoretical mirror reflectivity > 99% over 294nm, 466nm, and 563nm respectively. The Ti:Sapphire SBR was measured with a microspectrophotometer (courtesy of Filmetrics, Inc.). SBRs for the Cr:Forsterite and EDF lasers were measured with an FTIR. All measurements reveal losses due to SBR absorption.

The SBR epilayers were grown using gas source molecular beam epitaxy on GaAs. SBRs were defined using photolithography and wet etchants and oxidized in a tube furnace from 400-435°C. To examine the extent of oxidation, cross-sectional images were obtained using scanning electron microscopy (SEM). Reflectivity measurements were obtained using Fourier-transform infrared (FTIR) spectroscopy and a microspectrophotometer. Pre-oxidation thicknesses were determined from FTIR spectroscopy and high-resolution x-ray diffraction rocking curves of unoxidized SBRs.

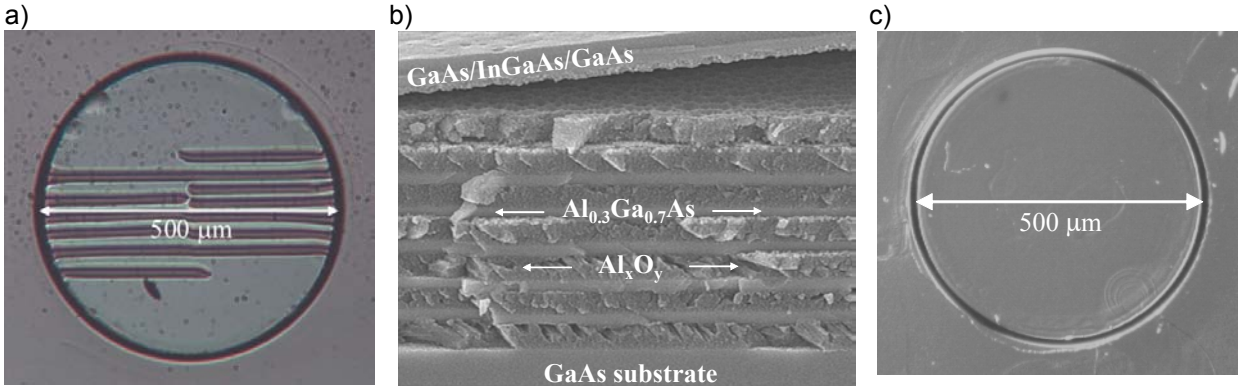

Figure 2. (a) Differential Interference Contrast (DIC) image of fully-oxidized SBR (420°C, 3.5hrs). (b) SEM image of SBR cross-section showing delamination of absorber layers: 52nm GaAs/80nm InGaAs/52nm GaAs with 7 pair $Al_xO_y/Al_{0.3}Ga_{0.7}As$ mirror stack (~194nm/100nm). (c) DIC image of SBR fully-oxidized using 50min. temperature ramp between 100°C and 410°C before and after oxidation (410°C, 4.5hrs).

Infrared SBRs are composed of $AlGaAs/Al_xO_y$ mirrors with InGaAs-based absorbers which strain the structure and, depending on the absorber thickness, may lead to delamination during the AlAs oxidation process. Figure 2(a) shows a plan view of a fully oxidized 500μm diameter SBR that is designed for operation at λ=1230nm. The cross-sectional view [Figure 2(b)] shows the delaminated absorber consisting of the highly strained 80nm thick InGaAs quantum well with GaAs cladding layers and a 7-pair $Al_{0.3}Ga_{0.7}As/Al_xO_y$ mirror stack. For oxidation temperatures between 410°C and 435°C, delamination occurs between the absorber and mirror layers. More severe delamination occurs at higher oxidation temperatures. In an alternate SBR design, the additional strain introduced by the InP cladding layers generally increases the observed amount of delamination. A controlled temperature ramp before and after oxidation has greatly reduced the delamination of the SBR structures despite the presence of strain [Figure 2(c)]. The oxidation temperature ramp allows the creation of large area, broadband SBRs with highly-strained absorbers for infrared lasers including an Er-doped fiber laser [4].

The same AlAs oxidation technique enables the fabrication of broadband SBRs at visible wavelengths. Using $In_{0.5}Ga_{0.15}Al_{0.35}P$, with a bandgap at 536nm and a index of refraction of ~3.1, as the high-index layer along with low-index Al_xO_y, Bragg mirrors are created for broadband reflection below 800nm. The top and side views of one structure are shown in Figure 3. Using a GaAs absorber layer, the as-grown structure is nominally unstrained and the oxidized structure may modelock a variety of lasers including Ti:Sapphire, Cr:LiSAF, Cr:LiCAF, and Cr:LiSGaF.

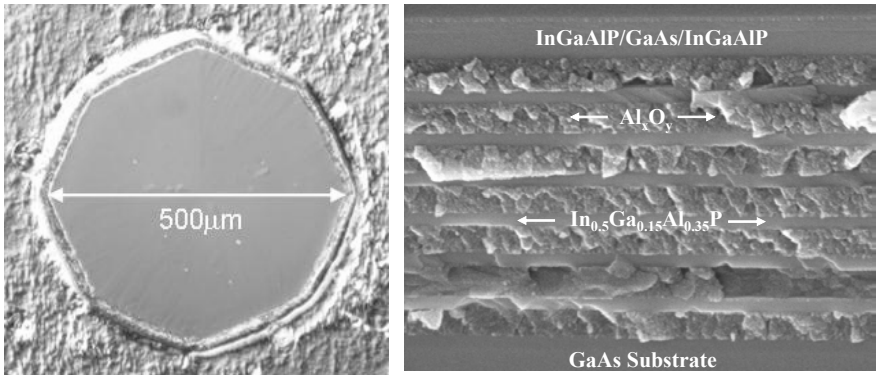

Figure 3. (a) Differential Interference Contrast (DIC) image of fully-oxidized SBR (410°C, 4.5hrs with temperature ramp). (b) SEM image of SBR cross-section showing 60 nm $In_{0.5}Ga_{0.15}Al_{0.35}P$, 10nm GaAs, 60 nm $In_{0.5}Ga_{0.15}Al_{0.35}P$ absorber with a 7 pair $In_{0.5}Ga_{0.15}Al_{0.35}P/Al_xO_y$ mirror stack (65nm/~135nm).

References

[1] Z. Zhang, T. Nakagawa, K. Torizuka , T. Sugaya, K. Kobayashi, "Gold-reflector-based semiconductor saturable absorber mirror for femtosecond mode-locked Cr4+:YAG lasers," Applied Physics B, 70, S59, 2000.

[2] M. Haiml, L. Gallmann, U. Keller, "GaAs absorber layer growth for broadband AlGaAs/fluoride SESAMs" Journal of Crystal Growth, 227-228, 172, 2001.

[3] T. R. Schibli, J. Kim, O. Kuzucu, J. T. Gopinath, S. N. Tandon, G. S. Petrich, L. A. Kolodziejski, J. G. Fujimoto, E. P. Ippen, and F. X. Kaertner. "Attosecond active synchronization of passively mode-locked lasers by balanced cross correlation." Optics Letters, 28 (2003) 947.

[4] J.W. Sickler, J.T. Gopinath, S.N. Tandon, H. Sotobayashi, G.S. Petrich, E.P. Ippen, and L.A. Kolodziejski. "Short-pulse laser using erbium-doped bismuth oxide fiber." CLEO 2004.

3. Super-collimation of Light within Photonic Crystal Slabs

Project Staff
Sheila N. Tandon, Marcus Dahlem, Peter Rakich, Mihai Ibanescu, Dr. Marin Soljacic, Dr. Gale S. Petrich, Professor Erich P. Ippen, Professor John D. Joannopoulos, Professor Henry I. Smith and Professor Leslie A. Kolodziejski

Sponsor
National Science Foundation Award Number DMR-02-13282

A super-collimator is a device in which light is guided by the dispersion properties of a photonic crystal slab rather than by photonic crystal defects or traditional waveguiding structures. Photonic crystals form the essence of the super-collimation effect. Being able to realize super-collimation would be potentially very useful for optical interconnects on planar lightwave circuits.

The device consists of a two-dimensional photonic crystal composed of a square lattice of cylindrical air holes etched into a high index material such as silicon. The top view schematic of the device shape with its cross-section is shown in Figure 1. The device consists of a cleaved sample with millimeter dimensions, with the photonic crystal (PC) occupying the entire surface of the super-collimator. The device was fabricated using silicon-on-insulator (SOI) wafers purchased from an outside vendor in which the low index insulator is used to minimize radiation loss into the high index substrate. The cleaved edges of the super-collimator function as input or output facets of the device. The initial design has focused on realizing super-collimation at a wavelength of 1.5 μm.

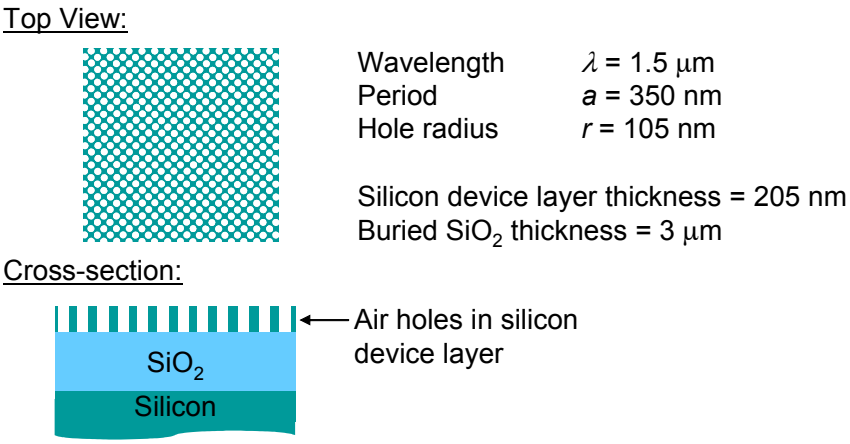

Figure 1. Super-collimator device design showing top and side views of the device.

The feature sizes of the photonic crystal can be scaled depending on the desired wavelength. A wavelength of 1.5μm implies a hole lattice constant of 350nm, and a hole radius of 105nm. The total thickness of the device (excluding substrate) is about 3.2 microns (205nm Si, 3μm SiO_2). Samples with varying sizes ranging from 3mm x 1cm to 1cm x 1cm were created.

The photonic crystal holes are patterned using interference lithography. After the lithography step, the photonic crystal holes are etched into a SiO_2 hard mask layer via reactive ion etching (RIE). The fully patterned hard mask layer is then used during the etch of the high index silicon layer via another RIE step.

Figure 2 shows images of the fabricated super-collimator. In the left inset to Figure 2, the full 1cm x 1cm device is shown with its cleaved input and output facets. The photonic crystal occupies the full sample area and the scanning electron microscopy (SEM) images at the center and right inset to Figure 2 show the details of the photonic crystal cross-section. The center image illustrates the large area nature of the

photonic crystal. The right inset shows air holes etched in silicon with a depth of 200 nm. The photonic crystal rests on a buried SiO_2 layer as shown.

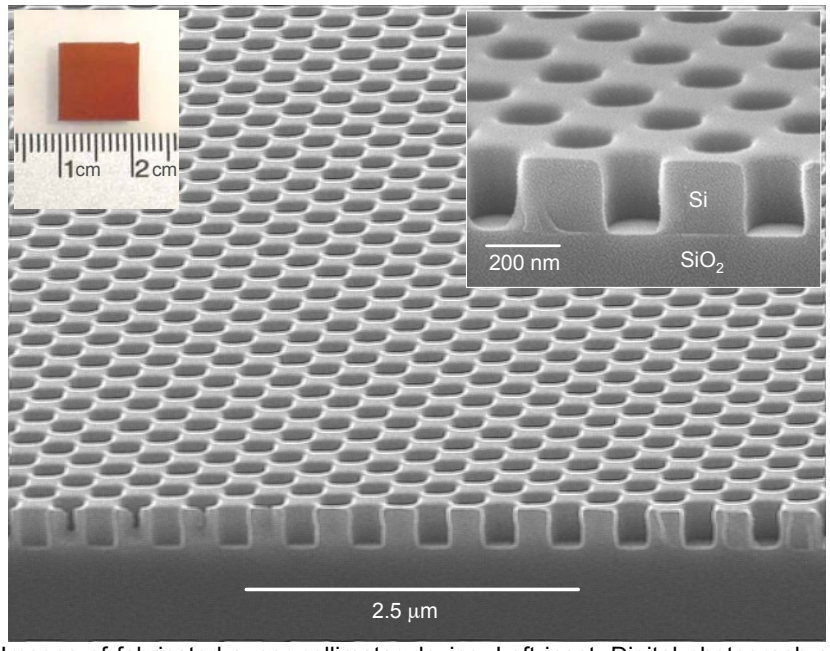

Figure 2. Images of fabricated super-collimator device. Left inset: Digital photograph showing full sample. Center: Scanning electron microscope (SEM) image showing large area 2D periodic photonic crystal. Right inset: SEM image showing cross-sectional image of the device fabricated using an SOI sample.

Testing of the super-collimator device is currently in progress in collaboration with the Ultra-fast Optics Group. Using an infrared camera, images of light propagation through the photonic crystal for a number of wavelengths could be observed from above the sample as shown in Figure 3. Each image represents a 250μm x 400μm area of the photonic crystal approximately 400μm from the input facet of the device. Figure 3 shows that at a wavelength of 1510nm, light propagation through the photonic crystal was indeed collimated as the light path resembles a stripe of light which propagates from the left to the right side of the imaging area. By tuning the wavelength of the input laser away from 1510nm, the beam no longer exhibits a collimated behavior and begins to diverge, with the beam width expanding as it propagates the length of the imaging area.

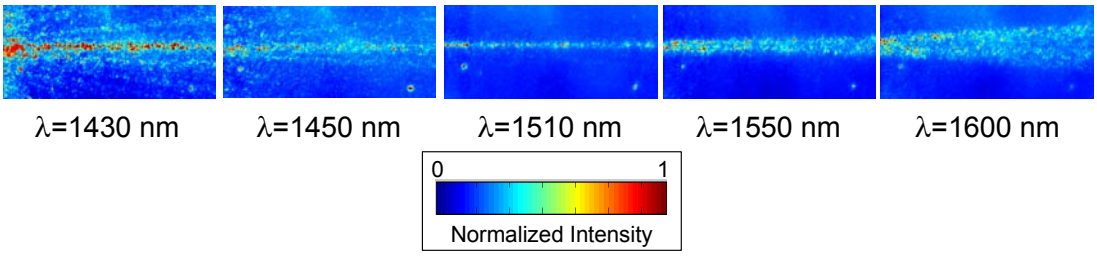

Figure 3. Infrared camera images showing the wavelength dependence of super-collimation at the top surface of the photonic crystal.

4. Nanomechanical Optical Switch for 1550nm Light

Project Staff
Reginald E. Bryant, Peter Rakich, Dr. Michelle L. Povinelli, Dr. Steven G. Johnson, Dr. Gale S. Petrich, Professor Erich P. Ippen, Professor John D. Joannopoulos, and Professor Leslie A. Kolodziejski

Sponsors:
National Science Foundation Award Number DMR-02-13282

One major objective of optical engineering research is to bring optical systems to the large-scale functionality of electrical systems. Striving to reach this objective, high-index-contrast, planar, evanescently-coupled, Nano-Electro-Mechanical (NEM) waveguide switches using the GaAs-based material system are being developed.

The concept that is behind the NEM switch combines two ideas: high-index-contrast waveguide optics and electromechanical actuation. High-index-contrast waveguide optics can route optical signals via waveguides with sizes of hundreds of nanometers in cross-section. Also, the evanescent method of energy transfer occurs along 100-nanometer coupling lengths and separations. The ability to exploit these length scales leads to a small device footprint, which lends itself to large-scale integrated optics. The physical dimensions of high-index-contrast evanescent coupling provide the impetus for the development of planar opto-electronic NEM systems. Furthermore, due to the size of NEM systems, it is possible to design switches with microsecond response times which would increase the number of potential applications for use by system designers that would not have been possible using the larger Micro-Electro-Mechanical-based switches.

A considerable amount of design and fabrication work has been invested in the development of the NEM switch. Theoretically, when a voltage is applied to the switch, the two waveguides reduce their separation distance in order to achieve lateral evanescent coupling, which allows 100% of the optical energy to be transferred between the waveguides. In the initial, unbiased state, the initial separation distance prevents lateral coupling. Experimentally, GaAs-based waveguides with release lengths over 30 microns long have been achieved for waveguides that are 1-μm thick and ~300-nm wide, with excellent lateral and horizontal waveguide-to-waveguide alignment. Because the GaAs waveguides typically reside on thermally-oxidized GaAlAs layers, oxidation experiments have been performed to investigate the correlation between the resulting stresses that affect the waveguide at the point where the waveguide becomes suspended to the stoichiometry of the oxidized GaAlAs layer.

5. Electrically-Activated Nanocavity Laser using One-Dimensional Photonic Crystals

Project Staff
Eric Mattson, Dr. Gale S. Petrich, and Professor Leslie A. Kolodziejski

Sponsors
National Science Foundation: Award Number DMR-02-13282

In the future, optical networks may play an expanded role not only in telecommunications, but also in computers and other common electronic devices. These optical networks will require small, on-chip light sources. Using the photonic crystal's ability to strongly confine light, photonic crystal lasers are both very small and very efficient, making them ideal for integration into photonic integrated circuits. The photonic crystal laser is electrically-activated, meaning that by simply applying a voltage to the device, light will be produced. The laser is very flexible in that by simply changing the active material or by changing the size and spacing of the holes that create the photonic crystal, the emission wavelength can be varied. This laser should be more efficient than the current light sources from the standpoints of energy and chip design, and should represent a major improvement in on-chip light sources.

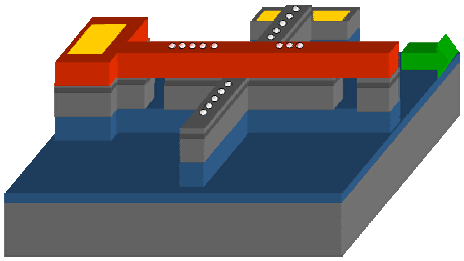

Figure 1. Depiction of the electrically-activated photonic crystal nanocavity laser. The green arrow represents the direction and location of the emitted light.

a) 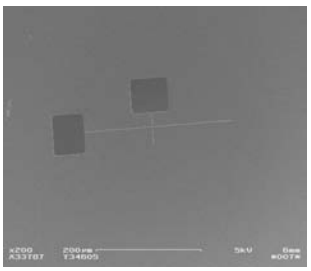 (b) 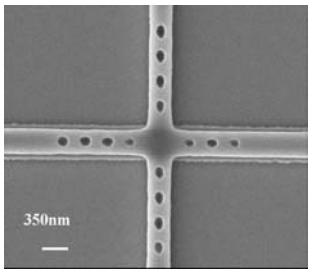

Figure 2. (a) SEM image of the crossing waveguide laser structure with contact pads, (b) magnified view of the intersection of the two waveguides, showing the holes that form the one-dimensional photonic crystals.

The laser consists of two one-dimensional photonic crystal waveguides that cross each other, shown in Figure 1. The laser's nanocavity which has a length of ~1μm is located where the defect regions of the two photonic crystal waveguides overlap. The bottom waveguide consists of an active layer containing InGaAs quantum dots, which emit at 1300nm, sandwiched between two GaAs and AlGaAs layers. The upper waveguide is composed of InGaAlP. Photons are generated in the quantum dot region of the nanocavity, and are confined laterally and vertically by index of refraction changes at the material's interfaces. At the two ends of the guide, a series of holes are etched, forming the photonic crystal, which confines the light lengthwise in the cavity. A small amount of light will leak from the lower AlGaAs waveguide into the upper InGaAlP waveguide. The upper waveguide exhibits less loss than the lower waveguide and has an asymmetric number of holes etched into it around the nanocavity, allowing the direction of the emitted light to be controlled. The entire photonic crystal part of the laser is about 5 μm square. Figure 2 (a) shows an scanning electronic microscopy image of the crossing waveguide structure and contact pads, and Figure 2 (b) shows the photonic crystal holes at the intersection of the two crossing waveguides.

Publications

Journal Articles, Published

S. N. Tandon, J.T. Gopinath, H.M. Shen, G.S. Petrich, L.A. Kolodziejski, F.X. Kaertner, and E.P. Ippen, "Large-area broadband saturable Bragg reflectors by use of oxidized AlAs." Optics Letters, 29(21), 2551-2553, November 2004.

S. N. Tandon, J. T. Gopinath, A. A. Erchak, G. S. Petrich, L. A. Kolodziejski, and E. P. Ippen, "Large Area Oxidation of AlAs Layers for Dielectric Stacks and Thick Buried Oxides." Journal of Electronic Materials, 33, 774-779, July 2004.

S. Assefa, P.T. Rakich, P. Bienstman, S.G. Johnson, G.S. Petrich, J.D. Joannopoulos, L.A. Kolodziejski, E.P. Ippen, and H.I. Smith, "Guiding 1.5μm light in photonic crystals based on dielectric rods," Appl. Phys. Lett. 85 (25), 6110-6112, December 2004.

S. Assefa, G.S. Petrich, L.A. Kolodziejski, M.K. Mondol, H.I. Smith, "Fabrication of photonic crystal waveguides composed of a square lattice of dielectric rods", J. Vac. Sci. Technol. B. 22(6) 3363-3365, Nov/Dec 2004.

Journal Articles, Submitted

S.N. Tandon, M. Soljacic, G.S. Petrich, J.D. Joannopoulos and L.A. Kolodziejski, "The Superprism Effect using Large Area 2D-Periodic Photonic Crystal Slabs." Photonics and Nanostructures. Accepted for publication, February 2005.

Meeting Papers, Published

S. N. Tandon, J.T. Gopinath, H.M. Shen, G.S. Petrich, L.A. Kolodziejski, F.X. Kaertner, and E.P. Ippen, "Broadband Saturable Bragg Reflectors from the Infrared to Visible using Oxidized AlAs." Proceedings of Conference on Lasers and Electro-Optics (CLEO), 2(2), 2004.

J.W. Sickler, J.T. Gopinath, S. N. Tandon, H. Sotobayashi, G.S. Petrich, E.P. Ippen, and L.A. Kolodziejski, "Femtosecond laser using broadband erbium-doped bismuth oxide gain fiber." Proceedings of Conference on Lasers and Electro-Optics (CLEO), 2(2) 2004.

S. Assefa, P.T. Rakich, P.P. Bienstman, S.G. Johnson, J.D. Joannopoulos, G.S. Petrich, L.A. Kolodziejski, E.P. Ippen, H.I. Smith, "Waveguiding in photonic crystals consisting of dielectric pillars near 1550 nm" Proceedings of Conference on Lasers and Electro-Optics (CLEO) 1(1), 2004.

S. Assefa, P.T. Rakich, M. Mondol, G.S. Petrich, L.A. Kolodziejski, E.P. Ippen, and H.I. Smith, "Fabrication of photonic crystal waveguides composed of a square lattice of dielectric rods," Electron, Ion and Photon Beam Technology and Nano Fabrication Conf. Proceedings, June 2004.

Meeting Papers, Submitted

H. Sotobayashi, J. T. Gopinath, E. M. Koontz, L. A. Kolodziejski and E. P. Ippen, “Wavelength Tunable Passively Modelocked Bismuth Oxide-based Erbium-doped Fiber Laser” Optics Communications 237(4-6), 399-403 July 2004.